arXiv:0811.3395v2 [math.GT] 23 Mar 2010

A COMBINATORIAL DESCRIPTION OF THE $U^2 = 0$ VERSION OF HEEGAARD FLOER HOMOLOGY

PETER S. OZSVÁTH, ANDRÁS I. STIPSICZ, AND ZOLTÁN SZABÓ

Abstract. We show that every 3–manifold admits a Heegaard diagram in which a truncated version of Heegaard Floer homology (when the holomorpic disks pass through the basepoints at most once) can be computed combinatorially.

1. Introduction

Heegaard Floer homology [13, 12] is a topological invariant for closed, oriented three-manifolds. These invariants are defined by considering versions of Lagrangian Floer homologies of certain tori (derived from Heegaard diagrams of Y) in a symmetric power of the Heegaard surface. There are several variants of these homology groups: there is a simple version $\widehat{\mathrm{HF}}(Y)$, where only those holomorphic disks are counted which are supported in the complement of a certain divisor in the symmetric power, and a richer version $\mathrm{HF}^-(Y)$, where the holomorphic disks passing through the above mentioned divisor are counted with weight, recorded in the exponent of a formal variable U. Specifically, this latter group admits the algebraic structure of an $\mathbb{F}[U]$–module, where $\mathbb{F} = \mathbb{Z}/2\mathbb{Z}$, and the corresponding $\widehat{\mathrm{HF}}$–theory can be derived from it by setting $U = 0$ at the chain complex level.

The computation of these invariants is typically challenging, since one needs to analyze moduli spaces of pseudo–holomorphic disks in high symmetric powers of the Heegaard surface. It was noticed by Sarkar and Wang [17] that for convenient Heegaard diagrams the complex analytic considerations are unnecessary for the purpose of calculating $\widehat{\mathrm{HF}}(Y)$. Specifically, the combinatorial structure of such a convenient diagram determines the chain complex computing the Heegaard Floer homology group $\widehat{\mathrm{HF}}(Y)$. In addition, Sarkar and Wang showed that any 3–manifold admits such a convenient Heegaard diagram (wich they called *nice*). In a related vein, [8] have used grid diagrams to calculate all the variants of Heegaard Floer homology of knots and links in S^3 in a purely combinatorial manner.

In this work we extend the result of Sarkar and Wang, by showing that for a suitably chosen Heegaard diagram the differential of the chain complex which counts holomorphic disks passing through the basepoint at most once (that is, the chain complex obtained

by setting $U^2 = 0$ in the chain complex computing $\mathrm{HF}^-(Y)$) can also be determined combinatorially. Furthermore, we show that every closed, oriented 3–manifold Y admits such a Heegaard diagram.

Indeed, letting $\mathrm{CF}^-(Y)$ denote the free $\mathbb{F}[U]$–module whose homology is the invariant $\mathrm{HF}^-(Y)$, and defining $\mathrm{HF}^-_{[n]}(Y)$ as the homology of the chain complex $(\mathrm{CF}^-(Y)/(U^n = 0), \partial^-)$, then we prove the following:

Theorem 1.1. *A closed, oriented 3–manifold Y admits a Heegaard diagram from which $\mathrm{HF}^-_{[2]}(Y)$, the specialization to $\mathbb{F}[U]/U^2$, can be computed in a purely combinatorial manner.*

A more precise version of our result is stated in Theorem 4.1, after we introduce the particular Heegaard diagram which is of use to us. For this diagram, the theorem then says that all non-negative domains of Whitney disks which have Maslov index one and which cross the distinguished divisor no more than once do, in fact, contribute with multiplicity one in the differential for $\mathrm{CF}^-_{[2]}(Y)$. Finding such domains is clearly a combinatorial matter. Our diagram is nice in the sense of Sarkar and Wang, hence for Whitney disks which are *disjoint* from the divisor, the result stated above actually follows from their work. The result is new for the case of disks which cross the distinguished divisor with multiplicity exactly one.

The Heegaard diagram considered in this paper is obtained from a triple branched cover of a link, represented by a grid diagram. As such, our constructions here were partly motivated by work of Levine [5], who studied branched covers of grid diagrams in a slightly different context. The construction of the Heegaard diagrams equips them with some extra structures, most notably with a projection to a grid diagram. This projection can be conveniently used in understanding properties of Maslov index zero and one homology classes.

The optimistic reader might hope that an analogous result — that non-negative, Maslov index one homology classes of Whitney disks for our Heegaard diagram always contribute with multiplicity one in the differential — could hold for disks which cross the distinguished divisor an arbitrary number of times. This fails, however, for our diagram already for the case where disks cross the basepoints with multiplicity two, i.e. for the $U^3 = 0$ version of the theory. Specifically, some Maslov index one, non-negative homology classes contribute to the differential, while others do not, and this choice is determined analytically. However, there is a way of formalizing this analytic choice combinatorially, and hence to come up with a concrete chain complex calculating $\mathrm{HF}^-_{[n]}(Y)$ for $n = 3$. We will return to this problem in [11].

The paper is organized as follows. In Section 2 we recall the basic notions regarding Heegaard Floer theory, while in Section 3 we describe the special type of Heegaard diagrams we would like to work with. In Section 4 we classify the Maslov index one

domains crossing the distinguished divisor at most once in the Heegaard diagram (these are the ones we encounter in determining the differential), and in Section 5 we determine the contribution of each Maslov index one domain in the differential, concluding the evaluation of $\mathrm{HF}^-_{[2]}(Y)$.

Acknowledgements: PSO was supported by NSF grant number DMS-0505811 and FRG-0244663. AS was supported by the Clay Mathematics Institute, by OTKA T49449 and by Marie Curie TOK project BudAlgGeo. ZSz was supported by NSF grant number DMS-0704053 and FRG-0244663.

2. Preliminaries

Heegaard Floer homologies. Suppose that the closed, oriented 3–manifold Y is given by a Heegaard diagram (Σ, α, β), where Σ is a surface with genus g, $\alpha = \{\alpha_1, \dots, \alpha_g\}$ and $\beta = \{\beta_1, \dots, \beta_g\}$ are two collections of disjoint, linearly independent, simple, closed curves on Σ with the property that the α_i's intersect the β_j's transversely. The 3–manifold Y can be reconstructed from the triple (Σ, α, β) by attaching 3–dimensional 2–handles along $\alpha_i \times \{-1\}$ and $\beta_j \times \{1\}$ to $\Sigma \times [-1, 1]$ and then attaching two 3–balls to the resulting 3–manifold with two S^2–boundaries. The α– (and similarly the β–) curves give rise to a torus $\mathbb{T}_\alpha$ (resp. $\mathbb{T}_\beta$) in the g^{th} symmetric power $\mathrm{Sym}^g(\Sigma)$ of Σ. Define $\mathrm{CF}^-(Y)$ as the free module over $\mathbb{F}[U]$ (with $\mathbb{F} = \mathbb{Z}/2\mathbb{Z}$) generated by the (finitely many) intersection points $\mathbb{T}_\alpha \cap \mathbb{T}_\beta$. Fix a point w on Σ which is in the complement of the α– and β–curves. The differential on $\mathrm{CF}^-(Y)$ is defined on an element $\mathbf{x} \in \mathbb{T}_\alpha \cap \mathbb{T}_\beta$ of the generating system by

$$\partial^- \mathbf{x} = \sum_{\mathbf{y} \in \mathbb{T}_\alpha \cap \mathbb{T}_\beta} \sum_{\phi \in \pi_2(\mathbf{x}, \mathbf{y}), \mu(\phi) = 1} \#\widehat{\mathcal{M}}(\phi) \cdot U^{n_w(\phi)} \mathbf{y}, \tag{2.1}$$

where $\pi_2(\mathbf{x}, \mathbf{y})$ denotes the space of homology classes of Whitney disks connecting $\mathbf{x}$ to $\mathbf{y} \in \mathbb{T}_\alpha \cap \mathbb{T}_\beta$, $\mu(\phi)$ denotes the Maslov index of the homology class ϕ, $n_w(\phi)$ is the algebraic intersection number of ϕ with the divisor $V_w = \{w\} \times \mathrm{Sym}^{g-1}(\Sigma) \subset \mathrm{Sym}^g(\Sigma)$, and $\widehat{\mathcal{M}}(\phi)$ is the quotient of the moduli space of holomorphic disks representing ϕ by the $\mathbb{R}$–action induced by translation, with respect to some suitably-chosen path of almost-complex structure J on the symmetric product. We typically suppress the choice of J from the notation; though the reader is cautioned that the actual differential typically does depend on this choice. Sometimes, when we wish to emphasize this choice, we include it in the notation for the moduli space, writing $\widehat{\mathcal{M}}_J(\phi)$ to denote the space of J-pseudo-holomorphic representatives of ϕ, modulo the $\mathbb{R}$–action. The term $\#\widehat{\mathcal{M}}(\phi)$ denotes the number of elements modulo 2 in the quotient space. The theory admits a sign refined version, which is defined over $\mathbb{Z}[U]$, but we will not address sign issues in this paper.

We can decompose $\Sigma - \alpha - \beta$ as a disjoint union of regions $\coprod_i D_i$ which we call *elementary domains*.

Definition 2.1. A homology class of Whitney disks $\phi \in \pi_2(\mathbf{x}, \mathbf{y})$ naturally determines a formal linear combination $D(\phi)$ of elementary domains by fixing a point d_i in each D_i and associating $\sum_i n_{d_i}(\phi) D_i$ to ϕ. The linear combination $D(\phi)$ is called the *domain associated to* ϕ. We say that ϕ is *non-negative* if all the coefficients $n_{d_i}(\phi)$ in the above sum are non-negative, and ϕ is *embedded* if each of the coefficients $n_{d_i}(\phi)$ in the above sum are either zero or one.

The sums in (2.1) defining the differential are not *a priori* finite for an arbitrary diagram. Finiteness is ensured, however, if we work with *admissible* diagrams (called *weakly admissible* in [13]) which we briefly recall here. A *periodic domain* for a Heegaard diagram is a two-chain with boundary among the α_i and β_j, and with local multiplicity zero at w. The space of periodic domains is an Abelian group, which is isomorphic to $H_2(Y; \mathbb{Z})$. A Heegaard diagram is *admissible* if every non-trivial periodic domain has both positive and negative local multiplicities. It turns out that this condition suffices to show that there are only finitely many non-zero terms with some fixed U-power appearing in $\partial^- \mathbf{x}$ in the sum of (2.1). To see then that the differential gives a well-defined polynomial in U (rather than a formal power series), we would require stronger notions of admissibility (this is *strong admissibility* of [13]; note that this notion depends also on a choice of background Spin^c structure). However, if we consider a variant of the theory (as we will do here) where we set $U^n = 0$ for some fixed $n \geq 1$, then the weak form of admissibility suffices to ensure that the sums are finite, so $(\mathrm{CF}^-(Y)/(U^n = 0), \partial^-)$ is a chain complex.

In [13] it is shown that the homology of the resulting chain complex is an invariant of the 3–manifold Y. A somewhat simpler version of the invariant can be given by setting $U = 0$, that is, considering the free group generated over $\mathbb{F}$ by $\mathbb{T}_\alpha \cap \mathbb{T}_\beta$ and counting holomorphic disks only if $n_w(\phi) = 0$, that is, the holomorphic disks avoid the divisor V_w.

More generally, fix an integer $n \geq 1$, consider the chain complex $(\mathrm{CF}^-(Y), \partial^-)$ and define

$$(\mathrm{CF}^-_{[n]}(Y), \partial^-) = (\mathrm{CF}^-(Y)/(U^n = 0), \partial^-).$$

The boundary operator on the quotient is denoted by the same symbol as on $\mathrm{CF}^-(Y)$; notice that the operator on the quotient counts holomorphic disks only when these pass through the basepoint at most $n - 1$ times. We denote the homology groups of this quotient complex by $\mathrm{HF}^-_{[n]}(Y)$. (In particular, it follows from the definition that $\mathrm{HF}^-_{[1]}(Y) = \widehat{\mathrm{HF}}(Y)$.) It is easy to see that the truncated groups $\mathrm{HF}^-_{[n]}(Y)$ are diffeomorphism invariants of Y. There is a splitting of Heegaard Floer homology indexed by

Spin^c structures, and in fact, this splitting is also a topological invariant of Y. We will not treat this Spin^c grading in the present paper.

The construction of Heegaard Floer homology can be extended to more general Heegaard diagrams, where the handle decomposition results from a Morse function with potentially more than one maximum and minimum. More specifically:

Definition 2.2. Let Σ be an oriented surface of genus g, equipped with a $(g+k-1)$-tuple of disjoint, embedded α–curves, the same number of disjoint, embedded β–curves, with the properties that

- the α-curves span a g–dimensional subspace of $H_1(\Sigma;\mathbb{Z})$, and
- the β-curves span another g–dimensional subspace of $H_1(\Sigma;\mathbb{Z})$.

This data specifies a three-manifold Y, and the tuple (Σ,α,β) is called an *extended Heegaard diagram for* Y. Suppose that we are given an extended Heegaard diagram as above so that we can also find k basepoints $w_1,\dots,w_k \in \Sigma - \alpha - \beta$, satisfying the following conditions:

- each of the k components of $\Sigma - \alpha$ contains exactly one of the basepoints in $\mathbf{w} = \{w_i\}_{i=1}^k$ and
- each of the k components of $\Sigma - \beta$ also contains exactly one of the basepoints $\mathbf{w} = \{w_i\}_{i=1}^k$.

Then, we call the tuple $(\Sigma,\alpha,\beta,\mathbf{w})$ a *multi-pointed Heegaard diagram for* Y.

Given a multi-pointed Heegaard diagram, we consider the chain complex over $\mathbb{F}[U]$ as before, endowed with the differential from Equation (2.1), where we use $n_w(\phi)$ to signify the sum $\sum_{i=1}^k n_{w_i}(\phi)$, compare [16]. We denote this complex by $\widetilde{\mathrm{CF}}^-(Y)$.

Lemma 2.3. *The homology groups of* $\widetilde{\mathrm{CF}}^-(Y)$ *determine* $\mathrm{HF}^-(Y)$ *by the formula*

$$H_*(\widetilde{\mathrm{CF}}^-(Y),\partial^-) \cong \mathrm{HF}^-(Y)\otimes H_*(T^{k-1}),$$

where T^{k-1} *is the torus of dimension* $k-1$*, with* k *denoting the number of basepoints. Similarly, for any integer* $n \geq 1$*, we have*

$$H_*(\widetilde{\mathrm{CF}}^-(Y)/(U^n=0),\partial^-) \cong \mathrm{HF}^-_{[n]}(Y)\otimes H_*(T^{k-1}).$$

Proof. In [16, Theorem 4.4] it is shown that $\mathrm{HF}^-(Y)$ can be calculated by a chain complex of the above type, except where there are k different variables U_i corresponding to the different basepoints. In the present context, we implicitly set all these variables equal to one another. The first isomorphism now follows from simple homological algebra (compare [9, Lemma 2.12]). The second isomorphism follows similarly. □

Maslov index formulae. In [6], Lipshitz developed a "cylindrical reformulation" of Heegaard Floer homology, where his differentials count certain pseudo-holomorphic curves in $[0,1]\times\mathbb{R}\times\Sigma$ satisfying appropriate asymptotic conditions, in place of holomorphic disks in the g-fold symmetric product of Σ. Using this reformulation, he deduces concrete formulae for the Maslov index of a homology class of Whitney disks in terms of combinatorial data on the Heegaard surface. We recall these here.

Suppose for simplicity that in our Heegaard diagram every elementary domain is a polygon. (By isotoping the β–curves this property can be easily achieved for any Heegaard diagram, cf. [17].) Then for every component D we can associate its *Euler measure* $e(D)$, which is equal to $1-\frac{m}{2}$ if D is a $2m$–gon. This quantity extends to formal linear combinations of the components: if $\phi\in\pi_2(\mathbf{x},\mathbf{y})$ is a given homology class of Whitney disks, then the Euler measure $e(\phi)$ of ϕ is equal to $e(D(\phi))=e(\sum n_iD_i)=\sum n_ie(D_i)$. The class $\phi\in\pi_2(\mathbf{x},\mathbf{y})$ also admits a *point measure*, which is defined as follows: Consider a corner point x_i of $D(\phi)$, i.e. a coordinate of $\mathbf{x}$ or $\mathbf{y}$. The average of the multiplicities of the four domains of $\Sigma-\alpha-\beta$ in $D(\phi)=\sum n_{d_i}(\phi)D_i$ meeting at x_i is the *local multiplicity of ϕ at x_i*, and the sum of these quantities for all coordinates of $\mathbf{x}$ and $\mathbf{y}$ gives the point measure $p(\phi)$ of $\phi\in\pi_2(\mathbf{x},\mathbf{y})$. It turns out that the Maslov index $\mu(\phi)$ can be conveniently expressed in terms of the Euler and point measures as follows:

Theorem 2.4. *(*[6, Corollary 4.3]*) If $\phi\in\pi_2(\mathbf{x},\mathbf{y})$ is a non-negative domain then $\mu(\phi)=e(\phi)+p(\phi)$.* □

For $\phi\in\pi_2(\mathbf{x},\mathbf{y})$ let $\Delta(\phi)$ denote the intersection number of ϕ with the diagonal $\Delta\subset\mathrm{Sym}^g(\Sigma_g)$. A formula similar to the one in Theorem 2.4 relates the Euler measure $e(\phi)$ to the Maslov index $\mu(\phi)$ with the help of the intersection number $\Delta(\phi)$:

Theorem 2.5. *(*[6]*) For a non-negative domain $\phi\in\pi_2(\mathbf{x},\mathbf{y})$ we have $\mu(\phi)=\Delta(\phi)+2e(\phi)$.* □

As we have already mentioned, the above results follow from the "cylindrical reformulation" of Heegaard Floer theory. We state another consequence of this theory which is of particular importance to us.

Theorem 2.6. *(*[6, Lemma 4.1]*) If $\phi\in\pi_2(\mathbf{x},\mathbf{y})$ is a non-negative homology class of Whitney disks, then there is an associated surface T decorated with $2g$ boundary points $\{p_i,q_i\}_{i=1}^g$ and a smooth map $u\colon T\longrightarrow\Sigma$ satisfying the following boundary conditions:*

- *The endpoints of the components of $\partial T-\{p_i,q_i\}_{i=1}^g$ are labelled with some p_i and q_i in an alternating manner.*
- *The image of $\{p_1,\dots,p_g\}$ is the tuple $\mathbf{x}$, while the image of $\{q_1,\dots,q_g\}$ is the tuple $\mathbf{y}$.*

- *Each component A of $\partial T - \{p_i, q_i\}_{i=1}^g$ which is oriented (with respect to the boundary orientation coming from T) as an arc from some p_i to some q_j is mapped into some α_i.*
- *Each component B of $\partial T - \{p_i, q_i\}_{i=1}^g$ which is oriented (with respect to the boundary orientation coming from T) as an arc from some q_i to some p_j is mapped into some β_i.*

Moreover,

- *The map u represents the two-chain associated to ϕ.*
- *Let d denote the number of coordinates of $\mathbf{x}$ where the local multiplicity of ϕ is non-zero; the remaining $g - d$ coordinates of $\mathbf{x}$ coincide with $g - d$ coordinates of $\mathbf{y}$. Then, our source surface T decomposes as the disjoint union $T = S \coprod P$, where P consists of a collection of $g - d$ disks which are mapped to Σ via constant maps. The Euler characteristic of S is determined by the homology class of ϕ by the formula*

$$\chi(S) = d - \Delta(\phi). \tag{2.2}$$

- *The map u, when restricted to S, is a branched cover onto its image.*

The above theorem is a consequence of the main result of [6], where (for suitable almost-complex structure) the pseudo-holomorphic disks in $\mathrm{Sym}^g(\Sigma)$ are identified with pseudo-holomorphic maps

$$v\colon S \longrightarrow [0,1] \times \Sigma \times \mathbb{R}.$$

The map u referred to in the statement of Theorem 2.6 is obtained from the map v by post-composing with the projection to Σ.

Note that the topology of S is not (necessarily) uniquely determined from the homology class of ϕ; however, according to Equation (2.2), its Euler characteristic is. Moreover, by Theorem 2.5 this expression can be turned into

$$\chi(S) = d - \mu(\phi) + 2e(\phi). \tag{2.3}$$

Let b denote the number of branch points of the branched cover map u when restricted to S. (Branch points on the boundary are counted with multiplicity $\frac{1}{2}$ each.) This number then can be computed by the following formula of [6, Proposition 4.2]:

$$b = \mu(\phi) - e(\phi) - \frac{1}{2}d. \tag{2.4}$$

Remark 2.7. Notice that when $d = 2p(\phi)$ then the above formula (together with Theorem 2.4) implies $b = 0$, hence in this case the map u is a local diffeomorphism.

3. Heegaard diagrams

In the present section, we describe the class of Heegaard diagrams used to establish Theorem 1.1. After introducing these diagrams, we collect some of their salient features.

A classical result of Hilden and Montesinos [4, 10] states that any closed, oriented 3–manifold Y can be presented as a simple 3–fold branched cover of S^3. Fix such a branched cover $\pi\colon Y \longrightarrow S^3$, and let $R_Y \subset S^3$ denote its branch set (or ramification set). The link R_Y (as any link in S^3) admits a *grid presentation*, cf. [1, 2, 3]. This means that S^3 admits a genus–one Heegaard diagram with n parallel curves $\mathbf{a} = \{\mathfrak{a}_i\}_{i=1}^n$ specifying one handlebody, and n parallel curves $\mathbf{b} = \{\mathfrak{b}_i\}_{i=1}^n$ orthogonal to the $\mathfrak{a}_i$, and with two distinguished points (one of them usually denoted by an O, the other one by an X) in every component of $T^2 - \mathbf{a}$ and of $T^2 - \mathbf{b}$. (In a subsequent construction we will enlarge both sets $\mathbf{a}$ and $\mathbf{b}$, but always so that curves in $\mathbf{a}$ are embedded and pairwise disjoint, and so are curves in $\mathbf{b}$.) The link can be recovered from this picture by connecting the O's to the X's in one handlebody and the X's to the O's in the other. Representing the torus by a square with its opposite sides identified, we can picture this on a square grid with an O and an X in each row and column, and R_Y is given by connecting the letters in the same row or column, with the convention that the vertical segment crosses over the horizontal one. Note that our notation here has slightly departed from the notation from Section 2, where $\mathbf{a}$ would have been denoted α and $\mathbf{b}$ would have been denoted β. We do this to reserve α and β for the Heegaard diagram for Y, rather than S^3. We denote the set of all the $O's$ and $X's$ by $\mathbf{O}$ and $\mathbf{X}$, respectively.

The simple triple branched cover along R_Y in its grid presentation gives a multi-pointed Heegaard diagram for Y as follows. Let $\Sigma \subset Y$ denote the inverse image of the Heegaard torus of S^3 under the triple branched covering. Since Σ is a simple 3–fold branched cover of the torus in $2n$ points, its genus is $n+1$. Since each $\mathbf{a}$-curve in the torus $T^2 \subset S^3$ bounds a disk in the corresponding handlebody, it lifts to three disjoint copies in Σ (and similarly for the $\mathbf{b}$–curves). An annular region $A_{i,i+1}$ between two neighboring $\mathbf{a}$–curves $\mathfrak{a}_i$ and $\mathfrak{a}_{i+1}$ in the grid diagram (containing two branch points) lifts to a two–component surface: one of the components is an annulus and the other is a 4–punctured sphere, as in Figure 1. For every such region $A_{i,i+1}$ in the torus $T^2 \subset S^3$ we introduce a new curve $\mathfrak{a}_{i+\frac{1}{2}} \subset A_{i,i+1}$, which we also include in the set of curves $\mathbf{a}$, and which is parallel (i.e. isotopic to, and disjoint from) both $\mathfrak{a}_i$ and $\mathfrak{a}_{i+1}$, but separates the two branch points in $A_{i,i+1}$, cf. Figure 2. Notice that there are two essentially different choices for such a curve, depending on the side of the new curve X (or O) is positioned. We can choose $\mathfrak{a}_{i+\frac{1}{2}}$ to be either of these two possible curves. The inverse image of this new curve in Σ has two components: one of these components is in the annular component of $\pi^{-1}(A_{i,i+1})$, while the other one (which double–covers $\mathfrak{a}_{i+\frac{1}{2}} \subset T^2$) is in the 4–punctured sphere component. This latter component obviously

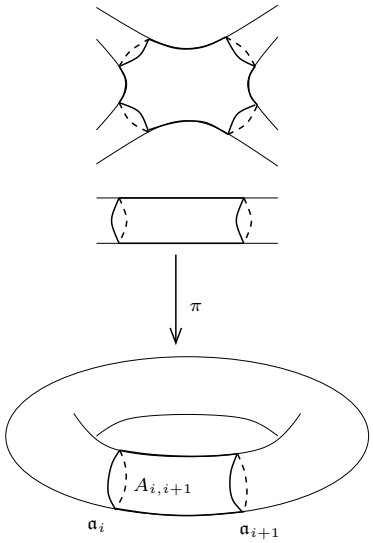

FIGURE 1. Domains in the Heegaard decomposition of the triple branched cover.

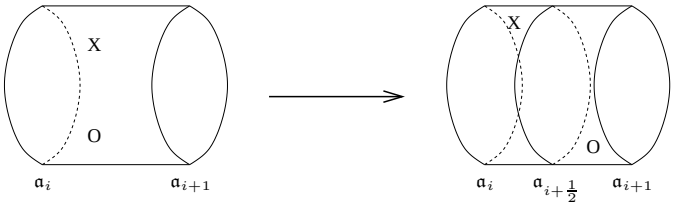

FIGURE 2. Introduction of a new α–curve.

separates the 4–punctured sphere into two pairs of pants, cf. Figure 3. We also add the similar half–indexed curves in the $\mathbf{b}$–direction. These newly chosen curves (as well as the corresponding circles in the Heegaard diagram for Y) will be referred to as *new curves in the grid diagram*, while the $\mathbf{a}$– and $\mathbf{b}$–curves in the original grid diagram for R_Y will be the *old curves*. We will call the grid diagram together with the new curves an *extended grid diagram*.

Consider now the extended grid diagram for R_Y. Both $\mathbf{a}$ and $\mathbf{b}$ partition the torus into $2n$ annuli, each annulus containing a single branch point, resulting in a $2n$–pointed Heegaard diagram for S^3. Clearly, every elementary domain in this diagram is a rectangle. Consequently, in the branched cover $(\Sigma, \pi^{-1}(\mathbf{a}), \pi^{-1}(\mathbf{b}))$ of the extended grid diagram (thought of as an extended Heegaard diagram for Y) every elementary domain is either an octagon (if it double covers an elementary rectangle with one X or an O in it), or otherwise it is a rectangle. To get a multi-pointed Heegaard diagram for Y (as required in the construction for Heegaard Floer homology), we have place basepoints in

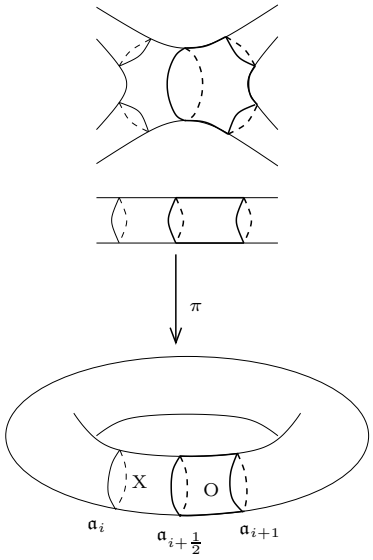

FIGURE 3. Domains in the Heegaard decomposition of the triple branched cover after introducing the new curves.

some of the elementary domains. By simply putting the basepoints into the octagons in Σ we do not get a multi-pointed Heegaard diagram, since not every component of the complement of the preimages of the $\mathbf{a}$– or the $\mathbf{b}$–curves contains a basepoint in this way: the annular components of $\pi^{-1}(A_{i,i+1})$ do not contain octagons, hence do not contain basepoints either. To fix this problem we could either put in more basepoints, or we could delete some curves in $\pi^{-1}(\mathbf{a})$ and $\pi^{-1}(\mathbf{b})$ to specify α and β. We choose to do the latter, by applying the following conventions: First, choose coherent orientations for the $\mathfrak{a}_i \in \mathbf{a}$ and the $\mathfrak{b}_j \in \mathbf{b}$, as specified by a basis $A, B \in H_1(T^2)$; i.e., for all $i = 1, \dots, n$, curves $\mathfrak{a}_i$ and $\mathfrak{b}_i$ (with suitable orientations) represent the homology class A and B respectively. Such a choice also induces a cyclic ordering on the curves in $\mathbf{a}$: the curve $\mathfrak{a}_{i+1}$ follows $\mathfrak{a}_i$ if the orientation on $\mathfrak{a}_{i+1}$, thought of as a boundary component of $A_{i,i+1} \subset T^2$ with its induced orientation, agrees with the orientation specified by A. The curve $\mathfrak{a}_{i+1}$ will be also called the *right* endcircle of the annulus $A_{i,i+1}$. We have an analogous cyclic ordering on the $\mathbf{b}$–curves. With this orientation convention in place, we refine our definition of a Heegaard diagram for Y as follows:

(1) For a new curve $\mathfrak{a}_{i+\frac{1}{2}}$ we consider only the component $\alpha_{i+\frac{1}{2}}$ of the inverse image of $\mathfrak{a}_{i+\frac{1}{2}}$ in Σ which double covers the curve downstairs (i.e., the one separating the 4–punctured sphere component into two pairs of pants). Similar choice applies for every new β–curve.
(2) For an old $\mathbf{a}$–curves we keep as α-curves only the two components of the inverse image of the *right* endcircle of the annulus $A_{i,i+1} \subset T^2 \subset S^3$ which are in the

4–punctured sphere (and do not consider the one in the annular component in $\pi^{-1}(A_{i,i+1})$). We apply the same principle to the β–circles.

Theorem 3.1. *The construction of Σ, α, β (as specified by the extended grid diagram $\mathbf{a}$, $\mathbf{b}$, and the basis $A, B \in H_1(T^2)$) together with a choice of k basepoints, one in each octogonal elementary domain, provides a multipunctured Heegaard diagram for Y.*

Proof. The pull-back of the grid diagram from S^3 along π obviously defines a Heegaard diagram of Y with Heegaard surface of genus $n+1$ and $3n$ α– and β–curves. Since the inverse images of the new curves all bound disks in the appropriate handlebody of the Heegaard decomposition of Y, by adding these curves we still have an extended Heegaard diagram of Y (now with $5n$ α– and β–curves). Since we deleted only curves which in homology linearly depended on the remaining curves, after the deletion we still have a Heegaard diagram for Y. The number of α–curves (and β–curves) in the resulting diagram is equal to $3n$, hence placing $2n$ basepoints we get a multi-pointed Heegaard diagram. The algorithm for deleting the curves is designed in such a way that the collection of the α–curves (and similarly the β–curves) gives a pair of pants decomposition of the Heegaard surface Σ. Since by construction each pair of pants contains a unique octagon, and we placed the basepoints exactly in the octagons, it follows that the result is a multi-pointed Heegaard diagram for Y. □

Definition 3.2. Given a simple 3–fold branched cover $\pi\colon Y \longrightarrow S^3$, fix an extended grid diagram $(T^2, \mathbf{a}, \mathbf{b}, \mathbf{O}, \mathbf{X})$ for the branch set R_Y of π in S^3, and a basis A, B for $H_1(T^2; \mathbb{Z})$ representing $\mathbf{a}$ and $\mathbf{b}$ respectively. According to Theorem 3.1, these choices determine a multi-pointed Heegaard diagram $(\Sigma, \alpha, \beta, \mathbf{w})$ for Y, which we call *adapted to the choices* or, when we wish to suppress the choices, simply an *adapted Heegaard diagram for Y*. In an adapted Heegaard diagram an α- or a β-curve is called a *new curve in Σ* if it projects onto a new curve in the extended grid diagram; otheriwse it is called an *old curve in Σ*. Sometimes, we drop the qualifier, and refer simply to *new curves* and *old curves*, when Σ is to be understood from the context.

Combining the above construction with the theorem of Hilden and Montesinos, we obtain the following:

Corollary 3.3. *Any closed, oriented 3–manifold admits an adapted Heegaard diagram.* □

The next proposition collects the most basic properties of adapted Heegaard diagrams. Further, more delicate properties of these diagrams (relevant to our subsequent discussions) will be discussed afterwards.

Proposition 3.4. *An adapted Heegaard diagram for Y satisfies the following properties:*

(1) *Every elementary domain in the Heegaard diagram is either a rectangle, which does not contain a basepoint, or it is an octagon, in which case it does contain a unique basepoint.*
(2) *Both the α– and β–curves give pair of pants decompositions of Σ; and each pair of pants contains a unique elementary domain which is an octagon (and all others are rectangles).*
(3) *Any two α– and β–curves meet either exactly once (this is guaranteed if at least one is an old curve), or exactly twice (which happens only when both are new curves), and in this latter case the two intersections come with equal signs.*
(4) *If $\mathbf{x}$ is a generator of $\mathrm{CF}^-(\Sigma,\alpha,\beta)$, then any curve $\mathfrak{a}\in\mathbf{a}\subset T^2$ meets the projection $\pi(\mathbf{x})$ of $\mathbf{x}$ in one or two points (counted with multiplicity). In the former case $\mathfrak{a}$ is a new curve while in latter case it is an old curve in the extended Heegaard diagram. Similar statement applies to the $\mathfrak{b}$–curves.*
(5) *Over every intersection point of some $\mathfrak{a}_i\in\mathbf{a}$ and $\mathfrak{b}_j\in\beta$ in the extended grid diagram there is either one or two intersection points of some α_k and β_ℓ in the adapted Heegaard diagram.*
(6) *The Heegaard diagram is admissible.*

Proof. The first five properties obviously follow from the definition of the Heegaard diagram. Notice that by Property (1) the Heegaard diagram we defined is nice in the sense of [17]. Property (6) then follows from [7, Corollary 3.2]. □

Next we discuss several further properties of this Heegaard diagram, which will be used in our arguments. In the proofs we will heavily use the extra structure an adapted Heegaard diagram admits, i.e. the extra restrictions imposed by the existence of the projection map from (Σ,α,β) to the extended grid diagram.

Lemma 3.5. *Let $a\subset\alpha_i$ be an arc in a new curve $\subset\Sigma$ with the property that π restricted to a is not injective. Then, there is an elementary domain on either side of a which contains a baspoint.*

Proof. By the assumption, the projection $\pi(a)$ is a full circle in the torus, i.e., the homology class $[\pi(a)]$ is equal to $\pm A$ (or $\pm B$). Therefore $\pi(a)$ has a rectangle on either of its sides which contains a basepoint. These rectangles lift to octagons containing basepoints as stated. □

Lemma 3.6. *Let $\phi\in\pi_2(\mathbf{x},\mathbf{y})$ be a non-negative homology class, and let $D=D(\phi)$ be its corresponding domain. Suppose that $a_1,a_2\subset\partial D$ are two arcs in ∂D which are contained in new curves α_1 and $\alpha_2\subset\Sigma$ respectively, and which have the property that the projection map π restricted to both a_1 and a_2 is not injective. Then, $n_w(\phi)\geq 2$.*

Proof. By Lemma 3.5 there are basepoints p_1 and p_2 in D adjacent to both a_1 and a_2, in the sense that there are elementary domains D_1 and D_2 appearing with non-zero

multiplicity in D, and D_i contains p_i and also an arc in a_i on its boundary. Since in the extended grid there is no elementary domain which has two arcs on its boundary from different new α–curves, the same holds in the adapted Heegaard diagram of Y. This shows that $D_1 \neq D_2$, implying that p_1 and p_2 are distinct, concluding the proof. □

There is a principle which is useful for excluding the existence of certain homology classes in an adapted Heegaard diagram, with specified local multiplicities at their corners. Since similar arguments will be repeatedly used in our latter discussions, we illustrate this principle in a particular case.

Lemma 3.7. *There is no homology class of Whitney disks $\phi \in \pi_2(\mathbf{x}, \mathbf{y})$ with the following properties:*

- *The homology class ϕ is non-negative,*
- *$n_w(\phi) \leq 1$,*
- *there are exactly two $\mathbf{x}$– and two $\mathbf{y}$–coordinates (x_1, x_2 and y_1, y_2) where the local multiplicity is non-zero,*
- *the local multiplicities at these four points are $\{\frac{1}{4}, \frac{1}{4}, \frac{3}{4}, \frac{3}{4}\}$ in some order,*
- *the points $\{x_1, y_1, x_2, y_2\}$ project to four distinct points on the torus, and*
- *all four points x_1, y_1, x_2, y_2 lie on a single component in the boundary of D.*

Proof. The local multiplicites in the four quadrants around a point of local multiplicity $\frac{3}{4}$ can distribute in two fundamentally different ways. They can be either $\{0, 1, 1, 1\}$, or they can be $\{0, 0, 1, 2\}$. (The third combinatorial possibility, $\{0, 0, 0, 3\}$, cannot occur since ϕ is a homology class of Whitney disks.) We exclude first the possibility that all local multiplicities around each corner point are ≤ 1, i.e. the case where the four multiplicities distribute as $\{0, 1, 1, 1\}$ around both points with multiplicity $\frac{3}{4}$.

We construct a closed, embedded, oriented path γ in the torus which goes through the projection of the four given points, consisting of arcs among the projections of the α_i and β_j, and turning 90° left or right depending on whether the corner point required to have local multiplicity $\frac{1}{4}$ or $\frac{3}{4}$, respectively. There are two combinatorially different cases for γ, according to the cyclic order of the different local multiplicities; these possibilities are illustrated in Figure 4. (The grid torus is given by the usual identification of opposite sides of the rectangles drawn.)

Note that γ does not *a priori* have to agree with the projection of the boundary of our domain D. However, it is easy to see that the projection of the boundary of D is necessarily gotten from γ by the following procedure: given any of the four turning points of γ, if we approach that corner of γ along some arc, then we can elongate that arc so that it goes around the torus (with the same orientation) more times.

As usual, let A and B denote two generators of $H_1(T^2; \mathbb{Z})$, where A is the homology class of the projection of an old curve α_i (with suitable orientation) while B is the

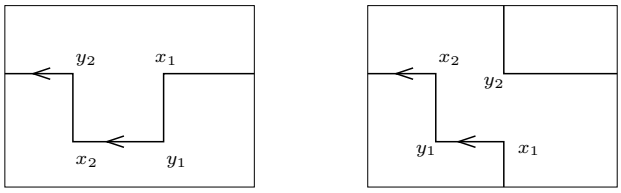

FIGURE 4. Choices of initial curve γ.

homology class of the projection of an old curve β_j. The possible choices of γ illustrated in Figure 4 show that γ represents either the homology class A, B (note that we are free to rotate the picture 90°), or $A+B$.

Consider the case where the homology class of γ is A. In this case, our allowed modification can add on some number of copies of $\pm B$, or alternatively some (non-negative) number of copies of A (but no copies of $-A$). Thus, this modification can never end up giving a null-homologous curve; on the other hand, the boundary of our domain must be null-homologous.

Similarly, in the case where the homology class of our curve γ is $A+B$, we can add on more copies of A and B (but not $-A$ or $-B$). Once again, we can never do this to achieve a curve which is null-homologous.

We have just excluded the possibility that the local multiplicities around both of the $\frac{3}{4}$ points are all ≤ 1 (and indeed, for that part of the argument, we have not yet used the hypothesis that $n_w(\phi) \leq 1$). Suppose now that at least one of these corner points has local multiplicities $\{0,0,1,2\}$. It follows readily that the other $\frac{3}{4}$ point has the same distribution of local multiplicities: the arc separating the region with multiplicity 2 from the adjacent region with multiplicity 0 appears with multiplicity 2 in the boundary, and this phenomenon does not occur for any other corner point whose local multiplicities are all ≤ 1 (but non-negative). Thus, it follows in fact that the two $\frac{3}{4}$ corners share an edge. That edge might be of type α or β: the two cases are the same (with a little change of notation), so we assume that latter.

In fact, we label coordinates as in Figure 5. The torus is divided into four regions, labelled W, X, Y, and Z. We label the adjoining curves in the extended Heegaard diagram a_1, a_2, b_1, b_2 (without regard to the earlier half-integral labeling). The points x_1 and y_1 have local multiplicity $\frac{3}{4}$, which distribute as $\{0,0,1,2\}$. In fact, the region around x_1 and y_1 with mulipliticty 2 project to W, while the region with multiplicity 1 around x_1 and y_1 project to X.

Let $a \subset \alpha_1$ be the arc from x_1 to y_2. We claim that this surjects onto $\mathfrak{a}_1$ in T^2. To see this, let ξ be the arc which is the top edge of W: it connects $\pi(x_1)$ to $\pi(y_2)$. Let $\widetilde{\xi}$ be the lift of ξ to Σ, so that its initial point is x_1, and we let its final point be denoted y.

The final point y is adjacent to a region with multiplicity 2 (the region projecting to W). It follows that y cannot be a corner point (the only corner points with multiplicity 2 in an adjacent region are x_1 and y_1), and hence a must be an arc in a new curve. Thus, the arc in the boundary of $D(\phi)$ connecting x_1 to y_2 must project to an arc in T^2 which covers the projection of x_1 twice. The same argument works for the arc connecting y_1 and x_2. In conclusion we found two arcs in $\partial D(\phi)$ which are contained by new α–curves and on which π is not injective. The application of Lemma 3.6 now provides the desired contradiction with the fact that $n_w(\phi) \leq 1$. □

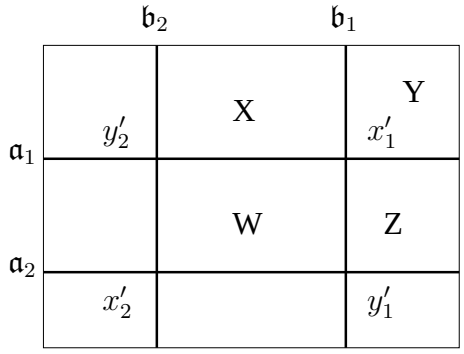

FIGURE 5. **Notation for the end of Lemma 3.7**. Here, we let x_i' be the projection of x_i and y_i' be the projection of y_i.

4. Non-negative domains with Maslov index one

We can now formulate a more precise version of Theorem 1.1, showing that $\mathrm{CF}^-_{[2]}(Y)$ can be determined combinatorially using an adapted Heegaard diagram for Y. The proof of the following theorem will rely on results of this and the subsequent sections and will be given at the end of Section 5.

Theorem 4.1. *Suppose that Y is given by an adapted Heegaard diagram. Then for any non-negative homology class ϕ with Maslov index $\mu(\phi) = 1$ and $n_w(\phi) = \sum n_{w_i}(\phi) \leq 1$, and for any choice of almost-complex structure J, the number $c(\phi, J) = \#\widehat{\mathcal{M}}(\phi)$ is equal to 1 modulo 2.*

The proof will start with the analysis of the possible non-negative domains with $n_w(\phi) \leq 1$ and with Maslov index zero. We will show that in an adapted Heegaard diagram, if ϕ satisfies these hypotheses, then it represents a constant map. From this (as it is shown by Proposition 4.2) it will follow that the contribution $c(\phi, J)$ of any homology class of Maslov index one to the differential is independent of the chosen almost–complex structure J. Afterwards, in Proposition 4.3, we place strong topological restrictions

on the possible homology classes of non-negative Whitney disks with Maslov index one and $n_w(\phi) \leq 1$. Indeed, with a little more work in Section 5, we are able to classify such domains, as stated in Theorem 5.1. We can then verify that the contributions of these domains are equal to 1 (mod 2). We begin with the promised analysis of Maslov index zero domains.

Proposition 4.2. *Suppose that Y is given by an adapted Heegaard diagram. Then for any non-negative domain $\phi \in \pi_2(\mathbf{x}, \mathbf{y})$ with Maslov index $\mu(\phi) = 1$ and $n_w(\phi) = \sum n_{w_i}(\phi) \leq 1$ the number $c(\phi, J) = \#\widehat{\mathcal{M}}(\phi)$ is independent of the chosen almost-complex structure J.*

Proof. The number $c(\phi, J)$ *a priori* might depend on the chosen almost-complex structure J. However, in that case, there must be a different, non-constant, non-negative homology class ψ of Whitney disks with $\mu(\psi) = 0$ with $n_w(\psi) \leq n_w(\phi)$. This can be seen from Gromov's compactness theorem: suppose that J_t is a generic one-parameter path of almost-complex structures connecting J_1 to J_2 (in fact, J_1 and J_2 are actually paths of almost-complex structures themselves, and hence J_t is really a path of paths), and consider the parameterized moduli space consisting of pairs (t, u) where $t \in [1, 2]$ and $u \in \widehat{\mathcal{M}}_{J_t}(\phi)$. This moduli space has boundary at $t = 1$, $t = 2$ (counted by the difference $c(\phi, J_1) - c(\phi, J_2)$), and further ends at splittings parameterized by triples t, u_1, u_2, where

- $t \in (1, 2)$,
- u_1 and u_2 are (non-constant) J_t-pseudo-holomorphic disks, and
- u_1 and u_2 represent homology classes ϕ_1 and ϕ_2 of Whitney disks, so that the juxtaposition of ϕ_1 and ϕ_2, $\phi_1 * \phi_2$ represents ϕ.

Moreover, by choosing our path generically, we can arrange that $\{\mu(\phi_1), \mu(\phi_2)\} = \{0, 1\}$. Thus, if $c(\phi, J_1) \neq c(\phi, J_2)$, there must be an end corresponding to a decomposition of ϕ. Our desired ψ is then either ϕ_1 or ϕ_2 (whichever has Maslov index equal to zero).

We now analyze non-negative domains with Maslov index 0 in our Heegaard diagram. We will show that such domain corresponds to a constant map, hence, according to the above said, we will verify that for each Maslov index one homology class of Whitney disks the quantity $c(\phi, J)$ is indepdent of J.

To this end, recall that $\mu(\psi) = e(\psi) + p(\psi)$ and by our assumption $n_w(\psi) \leq 1$. This implies that the domain of ψ contains at most one octagon with multiplicity at most one, hence $e(\psi) \geq -1$. Notice that in an adapted Heegaard diagram every domain has integral Euler measure, hence $e(\psi)$ is also an integer. If ψ is non-constant, we have that $p(\psi) > 0$. Since $\mu(\psi) = 0$ and $n_w(\psi) \leq 1$, it follows that $e(\psi) = -1$ and $p(\psi) = 1$.

Therefore a non-negative domain with $n_w(\psi) \leq 1$ and $\mu(\psi) = 0$ has $\Delta(\psi) = 2$ and $d \leq 2$.

In the case where $d = 1$, the possible local multiplicities of $\mathbf{x}$ and $\mathbf{y}$ are $(\frac{1}{4}, \frac{3}{4})$ and $(\frac{1}{2}, \frac{1}{2})$. In both cases the projection of the image of the boundary represents a nontrivial homology class in T^2, leading to a contradiction as follows. In the first case, the distinct coordinates of $\mathbf{x}$ and $\mathbf{y}$ are the two intersection points of a pair of new $\alpha-$ and $\beta-$ curves, hence the projection of the boundary represents $\pm A \pm B$ in $H_1(Y; \mathbb{Z})$. If the local multiplicities are given by $(\frac{1}{2}, \frac{1}{2})$ then ∂S maps to a complete $\alpha-$ or $\beta-$circle, hence the projection of the image of ∂S represents $\pm A$ or $\pm 2A$ (or $\pm B, \pm 2B$) in the homology of the torus. In both cases, $\pi(u(\partial S))$ is not null-homologous, providing a contradiction to the possibility that $d = 1$.

In the case where $d = 2$, the local multiplicities must be equal to $(\frac{1}{4}, \frac{1}{4}, \frac{1}{4}, \frac{1}{4})$ and the Euler characteristic of the surface S (given as in Theorem 2.6) is 0. Hence the domain must have two boundary components, each made out of an $\alpha-$ and a $\beta-$arc, intersecting each other twice. Since the local multiplicities are all equal to $\frac{1}{4}$, the two points must be distinct, hence the boundary arcs are all in new curves and the projection map on any of the boundary arcs is not injective. This means that the assumptions of Lemma 3.6 are satisfied, implying $n_w(\psi) \geq 2$, contradicting our assumption $n_w(\psi) \leq 1$. In summary, we have showed that there is no non-constant, non-negative domain ψ with $n_w(\psi) \leq 1$ and $\mu(\psi) = 0$ in our Heegaard diagram, which observation concludes the proof of the proposition. □

The next result provides a strong restriction on non-negative domains with Maslov index one in adapted Heegaard diagrams.

Proposition 4.3. *Let $\phi \in \pi_2(\mathbf{x}, \mathbf{y})$ be any non-negative domain with Maslov index one and $n_w(\phi) \leq 1$. Then the associated domain D of ϕ is the immersed image of either*

(A) a rectangle,
(B) a rectangle with a disk removed, or
(C) an octagon.

Moreover, in Cases (A) and (C), the local multiplicities at all the coordinates of $\mathbf{x}$ and $\mathbf{y}$ are 0 or $\frac{1}{4}$, while in Case (B) there is a single coordinate $p \in \mathbf{x} \cap \mathbf{y}$ where the local multiplicity is $\frac{1}{2}$, and at all other coordinates the local multiplicities are 0 or $\frac{1}{4}$.

Proof. Since all elementary domains which do not contain basepoints are rectangles, the argument of [17] applies, showing that the domain associated to any Maslov index one Whitney disk ϕ with $n_w(\phi) = 0$ is an embedded rectangle, and in fact all the local multiplicities at $\mathbf{x} \cup \mathbf{y}$ are $\leq \frac{1}{4}$. (In fact, for adapted diagrams this can be seen more directly; see the proof of Proposition 5.2 below.) This is Case (A) above.

If we consider $n_w(\phi) = 1$, then the Euler measure $e(\phi)$ is -1 (since the domain contains a unique octagon and some number of rectangles), so since $\mu(\phi) = 1$, it follows that point measure $p(\phi)$ must be equal to 2. From the equation $\mu(\phi) = \Delta(\phi) + 2e(\phi)$ we deduce $\Delta(\phi) = 3$. Furthermore, the Euler characteristic of the surface S associated to ϕ (as in Theorem 2.6) is given by Equation (2.3) as

$$\chi(S) = d - 3.$$

Since $p(\phi) = 2$ implies that there are at most 8 coordinates in $\mathbf{x} \cup \mathbf{y}$ with non-zero local multiplicities, we get that $d \leq 4$. Consequently there are several cases to consider according to the possible values of d:

Case I: $d = 1$

This case can be easily excluded, since by $d = 1$ there are only 2 coordinates with non-zero local multiplicity, hence the surface S has connected boundary. On the other hand, Equation (2.3) forces $\chi(S)$ to be -2 (implying the existence of an even number of boundary components), giving a contradiction.

Case II: $d = 2$

We claim that there are no domains with $\mu(\phi) = 1$, $n_w(\phi) = 1$, and $d = 2$ in an adapted Heegaard diagram. The argument proceeds by a case-by-case check. Notice first that when $d = 2$, the Euler characteristic of the surface S is equal to -1, hence it has an odd number of boundary components, which in this case can be only one. Since $d = 2$, there are four corner points, and each comes with a local multiplicity of at least $\frac{1}{4}$. Furthermore, the sum of the local multiplicities is equal to 2. Thus, the local multiplicities can distribute over these four points according to the following five possible ways:

(II.1) $(1, \frac{1}{2}, \frac{1}{4}, \frac{1}{4})$
(II.2) $(\frac{3}{4}, \frac{1}{2}, \frac{1}{2}, \frac{1}{4})$
(II.3) $(\frac{1}{2}, \frac{1}{2}, \frac{1}{2}, \frac{1}{2})$
(II.4) $(\frac{3}{4}, \frac{3}{4}, \frac{1}{4}, \frac{1}{4})$
(II.5) $(\frac{5}{4}, \frac{1}{4}, \frac{1}{4}, \frac{1}{4})$.

Case (II.1) does not exist, since if there is an $\mathbf{x}$–coordinate with local multiplicity 1, then there should be a similar $\mathbf{y}$–coordinate. Cases (II.2) and (II.3) are impossible since a pair of $\mathbf{x}$– and $\mathbf{y}$–coordinates with local multiplicity $\frac{1}{2}$ require an entire boundary component, but in our case the boundary is connected.

To exclude Case (II.4) first we show that the corner points must project onto four distinct points on the torus. Indeed, by Property (5) of Proposition 3.4 the corner points could *a priori* project to either two, three, or four points. If the projection consists of two points, then it is easy to see that both points lie on the same projected

α_i or β_j. Assume without loss of generality that they lie on the same projected α_i. Then they lie on different projected β_j, for which the projection π is obviously not injective, and hence Lemma 3.6 applies and provides a contradiction to $n_w(\phi) \leq 1$. The case where the projection consists of three points is excluded by Property (4) given in Proposition 3.4. Specifically, in this case it is easy to see that there must be some α_i or β_j whose projection contains a corner point with multiplicity one, although Property (4) cited above obviously implies that the total multiplicity of corner points on the projection of each α_i and β_j must be even. We are left with the possibility that the four corners project to four distinct points on the torus. This case, however, is exactly the one handled by Lemma 3.7, concluding the discussion of case (II.4).

Case (II.5) can be excluded by analyzing the projection of the boundary of the domain again. First, observe that if we consider the corner point of multiplicity $\frac{5}{4}$, then that must have some adjoining region with local multiplicity at least 2. Following the region with multiplicity 2 α-curve, we arrive at another corner which has no adjoining region with local multiplicity 2; it follows easily that the α–curve had to be a new curve. Similarly for the adjoining β–curve. Bearing this fact in mind, we project the four corners down to the torus. The corner points (as before) project to either two, three, or four distinct points on the torus. The case of two and three points can be excluded exactly as before. Consider now the possibility that the corner points have four distinct projections, which we denote by $\{\pi(x_1), \pi(y_1), \pi(x_2), \pi(y_2)\}$. Furthermore, let a_1, a_2, b_1, b_2 denote the four sides of the image of the rectangle S with a map u representing ϕ. According to Lemma 3.6 the projection π must be injective either on a_1 or on a_2 (and similarly either on b_1 or on b_2). If π on a_1 is not injective (but it is on a_2), then the projection of the image of ∂S will have non-trivial A-component in the homology of the torus, which would contradict the fact that this projection is null-homologous. A similar observation applies to the b–sides, implying at the end that the projection of the boundary of $u(S)$ is an embedded (null-homologous) curve in T^2. Thus, taking its complement, we see that Σ is divided into two regions where the local multiplicities are locally constant. But at the four corners we see at least three distinct local multiplicities, providing a contradiction.

Case III: $d = 3$

In this case, the surface S has vanishing Euler characteristic, hence an even number of boundary components, which number (by $d = 3$) is equal to two. Thus, the surface is an annulus. On one boundary component there are two corner points, and all the remaining four are on the other component. Regarding possible local multiplicities, there are two cases to distinguish:

(III.1): $(\frac{3}{4}, \frac{1}{4}, \frac{1}{4}, \frac{1}{4}, \frac{1}{4}, \frac{1}{4})$, and

(III.2): $(\frac{1}{2}, \frac{1}{2}, \frac{1}{4}, \frac{1}{4}, \frac{1}{4}, \frac{1}{4})$.

We discuss possibilities in **(III.1)** first. The boundary component with two corners consists of two curves intersecting each other twice, hence the arcs are in new curves and the projection map π is not injective on these arcs. In addition, their projection in the torus represents the homology class $\pm A \pm B$. Now π is either non-injective on one of the arcs in the rectangular boundary component (in which case Lemma 3.6 delivers a contradiction to $n_w(\phi) \leq 1$), or π is injective on the rectangular boundary, consequently the projection of this boundary component represents zero in the homology of the torus. Since the difference of the homology classes represented by the projections of the two boundary components must vanish, we arrived to a contradiction, showing that an adapted Heegaard diagram does not contain domains encountered in Case **(III.1)**.

In case **(III.2)** the two points with multipicity $\frac{1}{2}$ must coincide, hence in particular they are on the same boundary component. Abstractly, the surface S from Theorem 2.6 is an annulus with four marked points on one component, and two on the other. For the component with two marked points, one of the arcs is mapped onto an entire α (or β) circle, while the other arc maps degree zero onto the corresponding β (or α) circle. Abstractly such a domain is illustrated in Figure 6; this is Case (B) in the proposition. Such domains can be found in adapted Heegaard diagrams, as indicated in Figure 7.

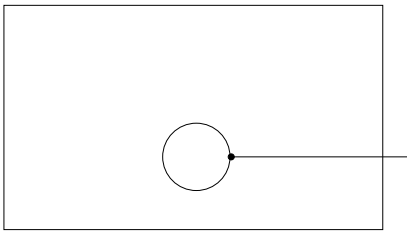

FIGURE 6. Schematic picture of domain in Case **(III.2)**.

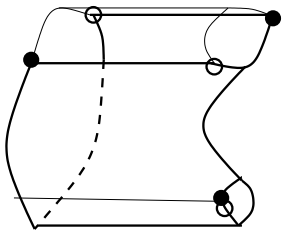

FIGURE 7. The realization of the domain of case **(III.2)** in an adapted Heegaard diagram.

Case IV: $d = 4$

When $d = 4$, there is only one possibility for the local multiplicities to sum up to 2: we must have eight corner points, each of local multiplicity $\frac{1}{4}$. Once again, the count of Euler characteristics and boundary components shows that there are two cases to consider: either the domain has three boundary components, or it has one. In the first case two boundary components consist of a pair of α– and β–circles, intersecting each other twice, hence admitting the property that π is not injective on them. The application of Lemma 3.6 (and the assumption $n_w(\phi) \leq 1$) then shows the nonexistence of this possibility. Therefore we are left with the case of a single boundary component and a surface of Euler characteristic 1, i.e., an octagon with local multiplicity $\frac{1}{4}$ at each of its eight corner points, giving Case (C), and concluding the proof of Proposition 4.3. Notice that by Equation (2.4) and Remark 2.7 in this case the map u given by Theorem 2.6 is a local diffeomorphism. □

5. Embeddedness of Maslov index 1 domains

Suppose that $\phi \in \pi_2(\mathbf{x}, \mathbf{y})$ is a homology class of Whitney disks with Maslov index 1 and $n_w(\phi) \leq 1$. According to Proposition 4.3, ϕ is represented by a domain which is the image (in the sense of Theorem 2.6) of a surface which is either a rectangle, an annulus of the shape given by Figure 6, or an octagon. The aim of the present section is to strenghten this result, by showing that in each of those cases, the domain is embedded (in the sense of Definition 2.1). The embeddedness of the domains will then allow us to compute $c(\phi)$ and conclude the proof of Theorem 4.1.

Theorem 5.1. *Let $\phi \in \pi_2(\mathbf{x}, \mathbf{y})$ be a non-negative homology class of Whitney disks in an adapted Heegaard diagram. Suppose moreover that ϕ has Maslov index one. If $n_w(\phi) = 0$, then*

- *ϕ is an embedded rectangle.*

If $n_w(\phi) = 1$, then once again ϕ is embedded. In fact, the domain of ϕ is one of the following two types of domain:

- *it is an annulus with four marked points x_1, y_1, x_2, y_3 on one boundary component, each of which has local multiplicity $\frac{1}{4}$, and one marked point $x_3 = y_3$ on the other, with local multiplicity $\frac{1}{2}$, or*
- *it is a disk with eight marked boundary points each with multiplicity $\frac{1}{4}$ (i.e. an octagon).*

The three cases above, of ourse, correspond to the to the three cases enumerated in Proposition 4.3. We subdivide the proof into the three cases.

Proposition 5.2. *(cf. also* [17]*) If ϕ is as in Proposition 4.3, and its domain is covered by Case (A) (i.e. it is an immersed rectangle), then the domain is embedded.*

Proof. Suppose that all the unmarked elementary domains in a multi-pointed Heegaard diagram are rectangles (or bigons), i.e., the Heegaard diagram is nice. Then, as in [17], all non-negative domains with Maslov index one and $n_w(\phi) = 0$ are rectangles (or bigons). In an adapted Heegaard diagram the argument is slightly simpler, in fact, we claim that for a rectangle D even the projection $\pi(\partial D)$ of the boudary ∂D into the grid diagram is embedded. Indeed, the argument used in proving cases (II.4) and (II.5) above applies and shows that the four corner points must project to four different points. Now if the projection π is not injective on a side a_1, then (in order $\pi(\partial S)$ to represent zero in homology) the same should hold for the opposite side a_2 (since all the local multiplicities are equal to $\frac{1}{4}$), which by Lemma 3.6 implies that $n_w(\phi) \geq 2$, contradiction our assumption. Thus, $\partial D \subset \Sigma$ is an embedded, null-homologous curve. As such, it divides Σ into two components where the local multiplicity is constant. Since there is one corner with local multiplicity $\frac{1}{4}$, these two constants are 0 and 1: i.e. the domain of ϕ is embedded. □

Proposition 5.3. *If ϕ is as in Proposition 4.3, and its domain falls under Case (B) (i.e. it is an immersed rectangle-minus-a-disk), then its domain is embedded.*

Proof. Suppose that $\phi \in \pi_2(\mathbf{x}, \mathbf{y})$ is a non-negative domain with Maslov index one, and S is an annulus (provided by Theorem 2.6) as indicated in Figure 6. Let $\gamma_1 \subset S$ denote the circular boundary component of the surafe, while $\gamma_2 \subset S$ the rectangular one.

Our first goal is to show that image $c_1 \cup c_2$ of $\gamma_1 \cup \gamma_2$ under the map u is an embedded one-manifold in Σ. Note that the curve γ_1 covers an α- or β-circle; the two cases are similar, so we assume the former, and write α_i for the α-circle covered by γ_1. Since α_i is a simple closed curve in Σ, and the local multiplicities in the corners on this boundary components are $\frac{1}{2}$, we get that $c_1 = u(\gamma_1)$ is an embedded curve. We claim that $c_2 = u(\gamma_2)$ is also an embedded curve in the Heegaard surface Σ. By the local multiplicities at the corner points it is obvious that u is injective on the corners of γ_2. In fact, the same argument shows that u is injective on each arc connecting two neighboring corner point. Consider the projection $\pi(c_2)$. The same analysis used earlier (for example, in excluding Case (II.4) in Proposition 4.3) shows that the four corner points on c_2 map to four different points under π. Since c_1 and c_2 are homologous to each other in Σ, we get that $\pi(c_1)$ is homologous to $\pi(c_2)$ in T^2, and $\pi(c_1)$ (as the image of an α–curve) has no B–component. Now if the projection is not injective on a boundary β–arc in c_2, then it is not injective on the other boundary β–arc as well (since the B–component of the homology class of T^2 determined by the projection of c_2 is 0), and so Lemma 3.6 applies again and gives a contradiction. Therefore π is injective on the β–sides of c_2, which now easily implies that c_2 is embedded in Σ.

Thus, the only remaining possible singularities in $c_1 \cup c_2$ are the intersection points between c_1 and c_2. The projections $\pi(c_1)$ and $\pi(c_2)$ can meet in at most two points p_1 and p_2, as it is illustrated in the second picture in Figure 8. However, in this case, we

claim that c_1 and c_2 are nonetheless disjoint: otherwise, there would be some region adjoining p_i where the multiplicity of the domain ϕ is 2. Considering the other corners of this region, we would be able to conclude also that the local multiplicity of ϕ at some region adjacent to one of the corners of ϕ is also 2, a contradition to our hypothesis on ϕ (according to which all local multiplicities of ϕ near its corner points are ≤ 1).

Now, $c_1 \cup c_2$ divides Σ into two components (since c_1 is homologically non-trivial even when projected to T^2, and c_2 is homologous to c_1), thus there are exactly two possible local multiplicities for any interior point in the domain of ϕ. Since near each corner point, both both 0 and 1 appear as local multiplicities, it follows that our domain ϕ is embedded. □

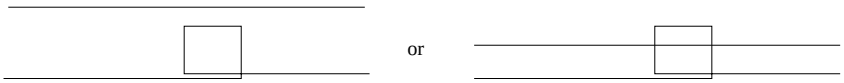

FIGURE 8. Possibilities for the projection of $\partial D(\phi)$ for a homology class ϕ is Case (B).

It remains to consider now Case (C), the case of octagons. The argument to verify this last case of Theorem 5.1 involves a case-by-case analysis. Before turning to this enumeration, we start with a simple result providing a condition for the boundary of an octagon to be embedded.

Lemma 5.4. *Suppose that $\phi \in \pi_2(\mathbf{x}, \mathbf{y})$ is a non-negative homology class of Whitney disks with Maslov index one in an adapted Heegaard diagram, and consider the corresponding map $u\colon S \to \Sigma$ from Theorem 2.6. Suppose moreover that u is not an embedding along ∂S. Then there is a vertex P of S and a point $x \in \partial S$ distinct from all the vertices such that $u(P) = u(x)$. In particular, $\partial D(\phi)$ contains at least one new α– and one new β–curve, on which the projection π is not injective.*

Proof. To set up notation, let the octagon S be as given by Figure 9, with the sides of it denoted by $a_1, \dots, a_4$ and $b_1, \dots, b_4$. Since by Equation (2.4) and Remark 2.7 the map $u\colon S \to \Sigma$ in this case is a local diffeomorphism, it equips S with a tiling (as in the proof of [17, Theorem 3.2], cf. also [6]). In our case, since we have $n_w(\phi) = 1$, the tiling will contain a single octagon and a number of rectangles. Let A_i denote the number of subintervals a side a_i is cut into by the β–curves, and define B_j similarly.

Suppose that u is not an embedding on ∂S, i.e. there is a point $x_0 \in a_1$ which maps to the same point as some $y_0 \in b_i$. If $i = 1$ (or $i = 4$), then the lemma is proved: if $u(x_0)$ and $u(y_0)$ are both intersections of α_1 and β_1 then (since these curves have exactly two intersections) one of them must be a corner point and the other one cannot be a corner point. (A similar argument applies for $i = 4$.) The arguments for $i = 2$ or $i = 3$ are symmetric, so we can assume that $i = 2$. The point y_0 now can move

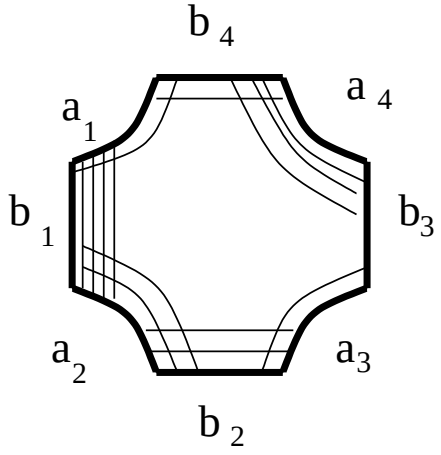

FIGURE 9. The octagon with the tiling.

along the preimage via u of an α–curve, intersecting b_2; on the tiling it either moves towards b_1 or b_3. Every step y_0 makes is mirrored by a step of x_0 on a_1. Since the local multiplicity of any corner point is $\frac{1}{4}$, in this procedure y_0 will reach b_1 or b_4 before x_0 moves to the endpoint of α_1. If y_0 reaches b_1, we get the desired second intersection of the image of a_1 and b_1, and the statement is proved. If it moves towards b_3, then it will take exactly A_3 steps before it reaches that boundary component, hence we conclude that $A_1 > A_3$. The terminal points of this procedure are denoted by x_1 and y_1 respectively. Now using the same principle for x_1 and y_1, by moving x_1 we either prove the statement (if x_1 moves towards a_4), or we get $B_1 < B_3$ and a new point pair x_2 and y_2 (now on a_2 and b_3). Repeating the same procedure, eventually we either get the desired configuration, or derive the inequality $A_3 > A_1$, which contradicts the inequality $A_1 > A_3$ found above. □

Now we are to discuss the last case in the proof of Theorem 5.1.

Proposition 5.5. *If ϕ is as in Proposition 4.3, and its domain falls under Case (C) (i.e. it is an immersed octagon), then its domain is embedded.*

Proof. Suppose now that $P_1, \dots, P_8$ denote the eight corners of the octagon, and for a map $u\colon S \to \Sigma$ representing ϕ, consider the points $u(P_i)$. Since the local multiplicity of each is equal to $\frac{1}{4}$, these points are all distinct. Define t_u as the cardinality of the set $\{\pi(u(P_i))\} \subset T^2$. Since any intersection point in the extended grid has at most two intersection point preimages in Σ, we get that t_u is between 4 and 8. As in the proof of Proposition 5.3, we start by showing that u is an embedding along ∂S. The somewhat lenghty argument is divided into cases acording to the value of t_u.

If $t_u = 4$ then there is no point which could play the role of x of Lemma 5.4, since x was not a corner, while the preimage of each $u(P_i)$ consists of only corners in this case. Said it in another way: the curves connecting the images must all be old curves (since they contain four coordinates of $\mathbf{x}$ and $\mathbf{y}$), but according to Lemma 5.4 the boundary ∂S is embedded if all the curves are old curves.

We exclude the possibility that $t_u = 5$ as follows. By Property (4) of Proposition 3.4, for the two intersection points $\mathbf{x}$ and $\mathbf{y}$ any curve in T^2 contains an even number of projections of coordinates. Now consider a point of the torus to which only one $u(P_i)$ projects. Consider either the α– or the β–curve passing through it, whichever does not contain the other point with a single preimage of the type $u(P_i)$. (Since there is only one further such point, there is a curve with this property.) Now this curve contains a single coordinate, plus the ones coming from the points having two preimages among the $u(P_i)$, changing the number of coordinates by 2. Therefore this number will have the wrong parity, concluding the analysis of the case $t_u = 5$.

Assume next that $t_u = 6$. In this case there are 4 points on the torus T^2 (which we will denote by Q_1, Q_2, Q_3, Q_4) with single preimages, and two (Q_5 and Q_6) with two preimages. The argument given above with the parities shows that Q_1, Q_2, Q_3, Q_4 must determine a rectangle in the grid, determining four curves $\mathfrak{a}_1, \mathfrak{a}_2$ and $\mathfrak{b}_1, \mathfrak{b}_2$. The last 2 points Q_5 and Q_6 must be on these four curves. If both Q_5, Q_6 are on $\mathfrak{a}$–curves (say, on $\mathfrak{a}_1$ and $\mathfrak{a}_2$) then they must share a $\mathfrak{b}$–curve, otherwise the $\mathfrak{b}$–curves on which they are located must be new curves in the grid diagram (since we need to pass from one sheet to the other on the curve), and the existence of two new curve segments in the boundary on which the projection is non-injective (by Lemma 3.6) contradicts $n_w(\phi) = 1$. Thus, the configuration should look like the one given in Figure 10(a). Now, however, the horizontal curves are old curves (since they carry 4 coordinates), hence ∂S must be embedded since there is no horizontal new curve in its image. There is a further case with $t_u = 6$ we have to consider, namely when Q_5 and Q_6 do not sit both on the $\mathfrak{a}$– or $\mathfrak{b}$–curves determined by the first four Q's. Such a situation is shown by Figure 10(b). Obviously the vertical curve passing through Q_5 (and the horizontal through Q_6) are new curves, while both curves passing through Q_2 are old (containing 4 coordinates in the projection). In order the boundary ∂S not to be embedded, we need two new curves, which intersect each other in a corner point and in a further boundary point. The only candidate in our picture for such curves are the two curves passing through Q_3. Since these must be parts of new curves with the property that π is not injective on them, considering them and the new curves through Q_5 and Q_6, Lemma 3.6 applies and delivers the required contradiction. This argument concludes the analysis of the case when $t_u = 6$, and shows that ∂S is embedded in this case.

When $t_u = 7$, there are three significantly different cases to consider. By $t_u = 7$ there is one point with two corner point preimages (symbolized by a circle on Figure 11)

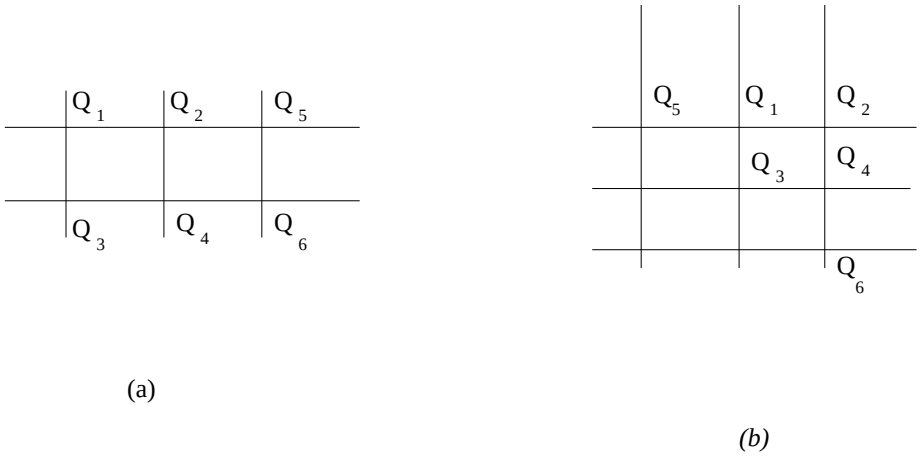

FIGURE 10. Two cases for $t_u = 6$.

and six with a single corner point preimage (denoted by x's). By cutting the torus along an appropriate pair of lines we can assume that the circle is in the upper left corner of the diagram. The circle must be connected to at least one of the x's, but the evenness of multiplicities along a line implies that there should be one more x on that line. Without loss of generality we can assume that these two x's are on a horizontal line passing through the circle. The orthogonal lines through these two x's must contain further x's, which are either in a single horizontal line, or on two distinct ones. If these two additional x's (x_3 and x_4) are on the same horizontal line, then the last two x's cannot be put down without violating the evenness condition. This shows that x_3 and x_4 are not on the same horizontal line. The last two x's must be on these two horizontal lines, and (again by the evenness condition) they should be in the same vertical one. This vertical line might be disjoint from the one passing through the circle (cf. Figure 11(a)), or is the one passing through the circled point (as it is given by Figures 11(b) and (c)). Notice that for Figure 11(a) there are furter combinatorial possibilities, but our subsequent argument will be insensitive for te further combinatorial distinction of these diagrams, hence we do not enumerate them.

In Figure 11(a) the vertical line passing through the circle is obviously a new curve and π is not injective on it. By Lemma 5.4 the boundary ∂S is embedded unless there is a horizontal and a vertical new curve which passes through one corner point and one other boundary point which is not a corner. If such a vertical new curve exists, it must be different from the one passing through the circled point, hence we get two parallel new curves, each having the property that the projection π is not injective on it, which (by Lemma 3.6) leads to a contradiction with the assumption $n_w(\phi) = 1$.

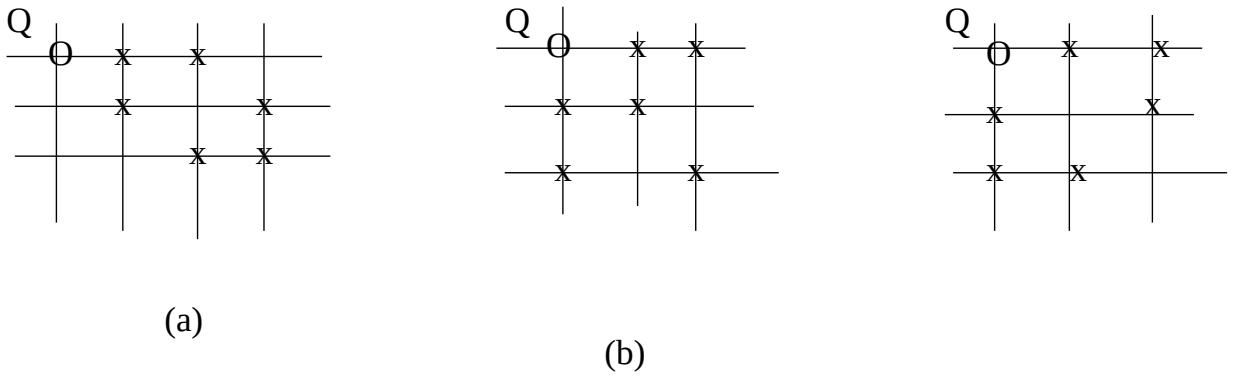

FIGURE 11. **Cases for $t_u = 7$.** Case (a) has six versions, by permuting the three vertical lines which do not contain O, but the various possibilities can be excluded by the same principle.

For the cases of Figures 11(b) and (c) we argue as follows: both curves passing through the circled point Q must be old (since the sum of the coordinates is equal to four). By traversing along the curves as $\pi(\partial(D(\phi)))$ does, the segments on these curves (two on each) are oriented in the same direction, and cannot perform complete turns because the local multiplicities are equal to $\frac{1}{4}$. The orientation of the image of $\partial(D(\phi))$ on both horizontal lines not passing through Q are opposite to the orientation we get on the line passing through Q. To verify these statements we have to cosnider all possible cases for the image of $\partial D(\phi)$. The combinatorial difference between Figures 11(b) and (c) *a priori* could mean that we get differente results in this oriantation issue, but the careful analysis of all cases shows that for both cases the statement above holds true. This implies that, in order to get a null–homologous curve, none of these curves can go around the torus (since they cannot cancel each other by the orientation reasoning). So even if one of the curves not passing through Q is a new curve, the projection π remains injective on it, so by Lemma 5.4 the boundary ∂S is embedded. This argument finishes the analysis when $t_u = 7$.

Assume finally that $t_u = 8$. Consider a curve passing through a chosen point $\pi(u(P_i))$. It contains an odd number of further such points, and obviously cannot contain more than three additional ones. Therefore we have to distinguish two cases:

(1) there is a line containing 4 points, or

(2) each line contains exactly 2.

In the first case, the perpendicular lines must contain an odd number of further points, hence that odd number must be one. The possibilities are pictured in Figure 12, since these additional four points then might lie on one or two lines, giving (i) and (iii). In

case (i) both horizontal lines are old curves (having four coordinates), hence there is no new horizontal curve in the diagram, which according to Lemma 5.4 implies that ∂S is embedded.

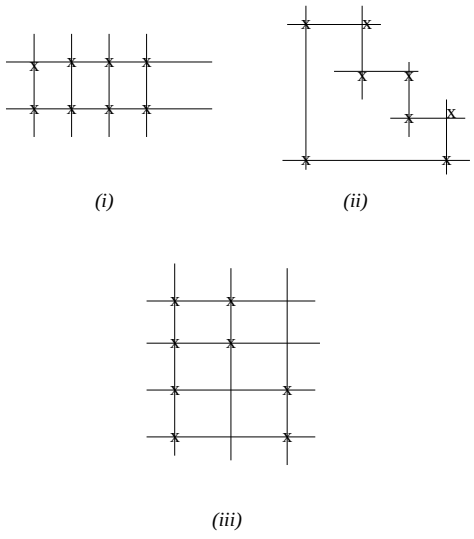

FIGURE 12. Three types of cases for $t_u = 8$.

In order to analyze possibilities regarding cases (ii) and (iii), we first prove a lemma. To state this result, suppose that the points $\pi(u(P_i))$ are given on the extended grid. In the spirit of Lemma 3.7, we specify how two neighbouring points can be connected with a short interval (for which we have four possibilities: there are two short intervals on the torus connecting two points, and each can be oriented in two ways). The initial choice creates a unique path, since when connecing all points we have to follow the convention that at every point we turn 90° to the left (dictated by the fact that the local multiplicity is $\frac{1}{4}$ at every point) and then use the short interval connecting the point to the next one. In this manner we get a closed curve γ in the extended grid, which might not be the projection of the image of ∂S in the Heegaard diagram, but it visits the corner points in the same order as the projection of $u(\partial S)$. As always, A and B will denote the homology generators of $H_1(T^2;\mathbb{Z})$. With these conventions in place now we are ready to state

Lemma 5.6. *Fix the images of the corner points of the octagon S. If for all four choices the homology class represented by the corresponding γ is different from $\pm A \pm B$ then any map $u\colon S \to \Sigma$ of an octagon representing $\phi \in \pi_2(\mathbf{x},\mathbf{y})$ with $\mu(\phi) = 1$ and with the given configuration of points $\pi(\phi(P_i))$ is an embedding on ∂S.*

Proof. Suppose that ∂S is not embedded, which by Lemma 5.4 implies, in particular, that there are new $\alpha-$ and $\beta-$curves such that their projections are not embedded. In order to recapture the image of ∂S from γ, therefore we must modify its homology class. Since we cannot alter the order and the turns, there is only one operation we can perform on γ: we can add to the short interval connecting two consecutive corners a complete turn, cf. the similar argument in Lemma 3.7. Notice that we cannot do it along an old curve (since this would increase the local multiplicity of the coordinates along that curve), and we cannot add two such twists along parallel new curves (cf. Lemma 3.6) or two turnes along the same curve. Thus, if ∂S is not embedded by u, we must change γ by $\pm A \pm B$ to get ∂S. Since the image of ∂S is nullhomologous, the claim follows. □

To apply this result, we need to list all possible projections of the 8 corner points, and compute the corresponding γ's. This is a fairly straightforward exercise. For case (iii) of Figure 12 there are two significantly different cases, all others can be derived by either switching the roles of the $\alpha-$ and $\beta-$curves or cutting the torus open to a rectangle along different lines. These two cases are shown by Figure 13. Each diagram

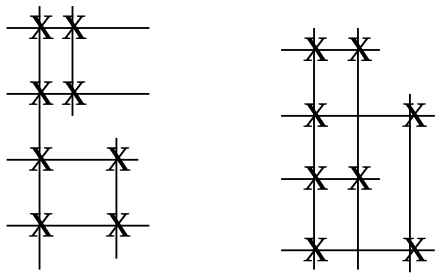

FIGURE 13. Two cases to consider for (iii).

gives rise to eight $\gamma-$curves. Specifically, the vertical segment of the γ curve through the upper-left x in each picture can be connected to one of two x's in the same vertical circle, with two possible orientations and in two possible ways. A simple case-by-case check shows that none of them is of the form $\pm A \pm B$; in fact, in all cases the homology of γ contains at most one of the factors $\pm A$ or $\pm B$.

The discussion of case (ii) of Figure 12 needs more cases to consider. First we list all possible configurations of the eight corner points in a 4×4 grid. It is easy to see that (when viewed on the torus) there is always a pair of points which are neighbours: if this does not hold, the boundary would fall into two components. We can assume that these two points are on the top left corner. By considering rotational and reflection symmetries (which obviously would provide similar results) there are four cases to consider,

and these configurations are shown by Figure 14. Remember that each configuration

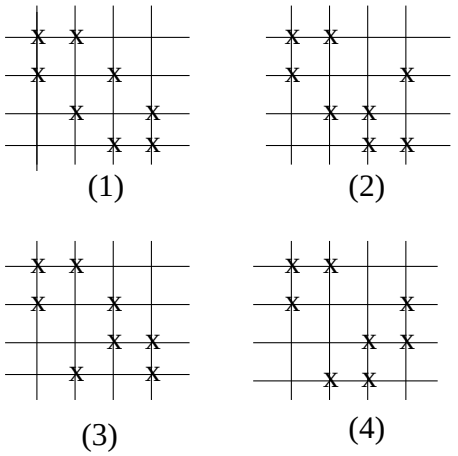

FIGURE 14. The four possibilities.

gives rise to four γ–curves, and it is not hard to check that for (1) the results are all null–homologous, and for (2) and (3) they represent $\pm A$ (or $\pm B$, depending on the chosen conventions). By Lemma 5.6 therefore in these cases the boundary ∂S is embedded. The configuration Figure 14(4), however, provides a curve γ with homology equal to $A + B$ (after appropriate orientations are fixed), hence the lemma itself is not enough to verify that ∂S is embedded. The four possible γ's are (up to symmetries) equivalent to the diagram shown in Figure 15. From γ we can actually recover the projection of

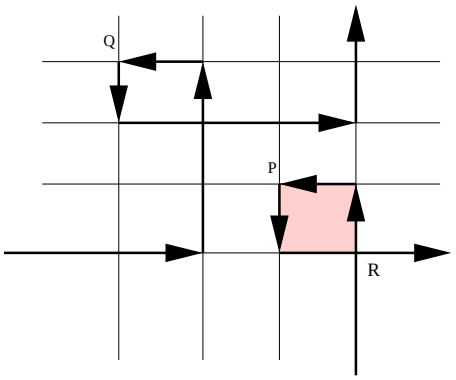

FIGURE 15. The curve γ when Lemma 5.6 does not apply.

∂S: since it bounds S it must be homologically trivial, turns as γ does, and cannot pass an old curve more than once (since the local multiplicities of the corners are equal

to $\frac{1}{4}$). To turn γ to a trivial element in the homology of the torus, we have to add a full turn both to the horizontal and to the vertical direction either at P or at Q; these possibilities are dictated by the orientation (as shown by Figure 15). If we add the horizontal and the vertical full turns in different points (one at P and the other one at Q), then by Lemma 5.4 the resulting image of ∂S comes from an embedded curve. If the two full twists are added at the same point, we need to argue further. The two choices as where to add the two full turns will provide similar results, so it is enough to examine the case when we do the modification at Q. Since these curves pass more than a complete turn down in the grid, these must be new curves (turning at least half), hence by Lemma 3.5 there are base points near them. Since we have a single base point in the domain, it must be in the square with vertex Q. Consider now the inverse images of the arcs passing through the point R. These arcs are disjoint in the Heegaard diagram for Y only if there is an octagon which projects onto the shaded region, contradicting the fact that the base point is in the elementary domain which projects to the rectangle adjacent to Q. On the other hand, if the arcs intersect, then a simple calculation of multiplicities shows that the domain to the lower right from R has multiplicity -1 (since the domain mapping to the shaded one in the grid has multiplicity 1), providing a contradiction to the fact that $d(\phi)$ is non-negative.

In conclusion, by examining all possible values of t_u we verified that the boundary of the surface S is embedded. Since it is a homologically trivial simple closed curve, its complement has two components, therefore in writing $D(\phi)$ as the formal linear combination of elementary domains we have only at most two distinct coefficients. Since the corner points have local multiplicities $\frac{1}{4}$, the domains around each corner point have multiplicities 0 or 1, hence the domain $D(\phi)$ is embedded (in the sense of Definition 2.1). □

The proof of the main theorem. After this case-by-case analysis we are ready to prove the main theorem of the paper.

Proof of Theorem 5.1. The classification of non-negative, Maslov index one domains with $n_w(\phi) \leq 1$ as stated in Theorem 5.1 is a consequence of Proposition 4.3, together with its strengthenings, Propositions 5.2, 5.3, and 5.5. □

Proof of Theorem 4.1. According to Theorem 5.1, if ϕ is a non-negative, Maslov index one domain with $n_w(\phi) \leq 1$, then it is one of three special types of domains; moreover, we know that $c(\phi)$ does not depend on a choice of almost-complex structure. We can now show for all three types of domains that $c(\phi) = 1$ holds, for example, as follows. We embed ϕ into a Heegaard diagram for S^3 for which there are three generators, in which ϕ is the non-negative domain which does not contain the basepoint. Since $\widehat{\mathrm{HF}}(S^3) = \mathbb{Z}/2\mathbb{Z}$, this Heegaard diagram shows that $c(\phi) = 1 \mod 2$. (For the case of the octagon, this is explictly done in [14, Theorem 6.1]; and a more general construction

is given in [15, Lemma 3.11] which handles all three cases.) Note that for the case of the annulus, the combinatorics of the diagram is important, in order for the answer to be independent of the choice of almost-complex structure. Since ϕ is embedded in the adapted Heegaard diagram for Y, its contribution $c(\phi)$ in the differential is the same as in the Heegaard diagram for S^3, concluding the proof. □

Proof of Theorem 1.1. According to Corollary 3.3, every three-manifold admits an adapted Heegaard diagram. According to Lemma 2.3, $\mathrm{HF}^-_{[2]}(Y)$ can be determined once one calculates $c(\phi)$ for every Maslov index one domain with $n_w(\phi) \leq 1$. According to Theorem 4.1, however, for such ϕ, we have that $c(\phi) = 1$ if and only if ϕ is non-negative. □

References

[1] J. S. Birman and W. W. Menasco. Special positions for essential tori in link complements. *Topology*, 33(3):525–556, 1994.

[2] H. Brunn. Über verknotete Kurven. *Verhandlungen des Internationalen Math. Kongresses (Zurich 1897)*, pages 256–259, 1898.

[3] P. R. Cromwell. Embedding knots and links in an open book. I. Basic properties. *Topology Appl.*, 64(1):37–58, 1995.

[4] H. M. Hilden. Every closed orientable 3-manifold is a 3-fold branched covering space of S^3. *Bull. Amer. Math. Soc.*, 80:1243–1244, 1974.

[5] A. Levine. Computing knot Floer homology in cyclic branched covers. arXiv:0709.1427.

[6] R. Lipshitz. A cylindrical reformulation of Heegaard Floer homology. *Geom. Topol.*, 10:955–1097 (electronic), 2006.

[7] R. Lipshitz, C. Manolescu, and J. Wang. Combinatorial cobordism maps in hat Heegaard Floer theory. *Duke Math. J.*, 145(2):207–247, 2008.

[8] C. Manolescu, P. S. Ozsváth, and S. Sarkar. A combinatorial description of knot Floer homology. To appear in *Ann. Math.*, arXiv:math/0607691.

[9] C. Manolescu, P. S. Ozsváth, Z. Szabó, and D. Thurston. On combinatorial link Floer homology. *Geom. Topol.*, 11:2339–2412, 2007.

[10] J. M. Montesinos. A representation of closed orientable 3-manifolds as 3-fold branched coverings of S^3. *Bull. Amer. Math. Soc.*, 80:845–846, 1974.

[11] P. S. Ozsváth, A. Stipsicz, and Z. Szabó. A combinatorial description of the $U^3 = 0$ version of Heegaard Floer homology. in preparation, 2008.

[12] P. S. Ozsváth and Z. Szabó. Holomorphic disks and three-manifold invariants: properties and applications. *Ann. of Math. (2)*, 159(3):1159–1245, 2004.

[13] P. S. Ozsváth and Z. Szabó. Holomorphic disks and topological invariants for closed three-manifolds. *Ann. of Math. (2)*, 159(3):1027–1158, 2004.

[14] P. S. Ozsváth and Z. Szabó. Knot Floer homology, genus bounds, and mutation. *Topology Appl.*, 141(1-3):59–85, 2004.

[15] P. S. Ozsváth and Z. Szabó. A cube of resolutions for knot Floer homology. arXiv:0707.1165, 2007.

[16] P. S. Ozsváth and Z. Szabó. Holomorphic disks, link invariants, and the multi-variable Alexander polynomial. *Alg. Geom. Topol.*, 8:615–692, 2008.

[17] S. Sarkar and J. Wang. An algorithm for computing some Heegaard Floer homologies. To appear in *Ann. Math.*, arXiv:math/0607777, 2006.

Department of Mathematics, Columbia University, New York, NY, 10027

E-mail address: petero@math.columbia.edu

Department of Mathematics, Columbia University, New York, NY, 10027 and, Rényi Institute of Mathematics, Budapest, Hungary

E-mail address: stipsicz@math-inst.hu

Department of Mathematics, Princeton University, Princeton, NJ, 08450

E-mail address: szabo@math.princeton.edu